Branching fraction measurements of χ_{c0} and χ_{c2} to $\pi^0\pi^0$ and $\eta\eta$

M. Ablikim[1], M. N. Achasov[5], L. An[9], Q. An[31], Z. H. An[1], J. Z. Bai[1], Y. Ban[18], N. Berger[1], J. M. Bian[1], I. Boyko[13], R. A. Briere[3], V. Bytev[13], X. Cai[1], G. F. Cao[1], X. X. Cao[1], J. F. Chang[1], G. Chelkov[13a], G. Chen[1], H. S. Chen[1], J. C. Chen[1], L. P. Chen[1], M. L. Chen[1], P. Chen[1], S. J. Chen[16], Y. B. Chen[1], Y. P. Chu[1], D. Cronin-Hennessy[30], H. L. Dai[1], J. P. Dai[1], D. Dedovich[13], Z. Y. Deng[1], I. Denysenko[13b], M. Destefanis[32], Y. Ding[14], L. Y. Dong[1], M. Y. Dong[1], S. X. Du[36], M. Y. Duan[21], J. Fang[1], C. Q. Feng[31], C. D. Fu[1], J. L. Fu[16], Y. Gao[27], C. Geng[31], K. Goetzen[7], W. X. Gong[1], M. Greco[32], S. Grishin[13], Y. T. Gu[9], A. Q. Guo[17], L. B. Guo[15], Y.P. Guo[17], S. Q. Han[15], F. A. Harris[29], K. L. He[1], M. He[1], Z. Y. He[17], Y. K. Heng[1], Z. L. Hou[1], H. M. Hu[1], J. F. Hu[6], T. Hu[1], X. W. Hu[16], B. Huang[1], G. M. Huang[11], J. S. Huang[10], X. T. Huang[20], Y. P. Huang[1], C. S. Ji[31], Q. Ji[1], X. B. Ji[1], X. L. Ji[1], L. K. Jia[1], L. L. Jiang[1], X. S. Jiang[1], J. B. Jiao[20], D. P. Jin[1], S. Jin[1], S. Komamiya[26], W. Kuehn[28], S. Lange[28], J. K. C. Leung[25], Cheng Li[31], Cui Li[31], D. M. Li[36], F. Li[1], G. Li[1], H. B. Li[1], J. Li[1], J. C. Li[1], Lei Li[1], Lu Li[1], Q. J. Li[1], W. D. Li[1], W. G. Li[1], X. L. Li[20], X. N. Li[1], X. Q. Li[17], X. R. Li[1], Y. X. Li[36], Z. B. Li[23], H. Liang[31], T. R. Liang[17], Y.T. Liang[28], Y. F. Liang[22], G. R Liao[8], X. T. Liao[1], B. J. Liu[24,25], C. L. Liu[3], C. X. Liu[1], C. Y. Liu[1], F. H. Liu[21], Fang Liu[1], Feng Liu[11], G. C. Liu[1], H. Liu[1], H. B. Liu[6], H. M. Liu[1], H. W. Liu[1], J. Liu[1], J. P. Liu[34], K. Liu[18], K. Y Liu[14], Q. Liu[29], S. B. Liu[31], X. H. Liu[1], Y. B. Liu[17], Y. F. Liu[17], Y. W. Liu[31], Yong Liu[1], Z. A. Liu[1], G. R. Lu[10], J. G. Lu[1], Q. W. Lu[21], X. R. Lu[6], Y. P. Lu[1], C. L. Luo[15], M. X. Luo[35], T. Luo[1], X. L. Luo[1], C. L. Ma[6], F. C. Ma[14], H. L. Ma[1], Q. M. Ma[1], X. Ma[1], X. Y. Ma[1], M. Maggiora[32], Y. J. Mao[18], Z. P. Mao[1], J. Min[1], X. H. Mo[1], N. Yu. Muchnoi[5], Y. Nefedov[13], F. P. Ning[21], S. L. Olsen[19], Q. Ouyang[1], M. Pelizaeus[2], K. Peters[7], J. L. Ping[15], R. G. Ping[1], R. Poling[30], C. S. J. Pun[25], M. Qi[16], S. Qian[1], C. F. Qiao[6], J. F. Qiu[1], G. Rong[1], X. D. Ruan[9], A. Sarantsev[13c], M. Shao[31], C. P. Shen[29], X. Y. Shen[1], H. Y. Sheng[1], S. Sonoda[26], S. Spataro[32], B. Spruck[28], D. H. Sun[1], G. X. Sun[1], J. F. Sun[10], S. S. Sun[1], X. D. Sun[1], Y. J. Sun[31], Y. Z. Sun[1], Z. J. Sun[1], Z. T. Sun[31], C. J. Tang[22], X. Tang[1], X. F. Tang[8], H. L. Tian[1], D. Toth[30], G. S. Varner[29], X. Wan[1], B. Q. Wang[18], J. K. Wang[1], K. Wang[1], L. L. Wang[4], L. S. Wang[1], P. Wang[1], P. L. Wang[1], Q. Wang[1], S. G. Wang[18], X. D. Wang[21], X. L. Wang[31], Y. D. Wang[31], Y. F. Wang[1],

Y. Q. Wang[20], Z. Wang[1], Z. G. Wang[1], Z. Y. Wang[1], D. H. Wei[8], S. P. Wen[1], U. Wiedner[2], L. H. Wu[1], N. Wu[1], W. Wu[14], Y. M. Wu[1], Z. Wu[1], Z. J. Xiao[15], Y. G. Xie[1], G. F. Xu[1], G. M. Xu[18], H. Xu[1], Min Xu[31], Ming Xu[9], X. P. Xu[11d], Y. Xu[17], Z. Z. Xu[31], Z. Xue[31], L. Yan[31], W. B. Yan[31], Y. H. Yan[12], H. X. Yang[1], M. Yang[1], P. Yang[17], S. M. Yang[1], Y. X. Yang[8], M. Ye[1], M.H. Ye[4], B. X. Yu[1], C. X. Yu[17], L. Yu[11], C. Z. Yuan[1], Y. Yuan[1], Y. Zeng[12], B. X. Zhang[1], B. Y. Zhang[1], C. C. Zhang[1], D. H. Zhang[1], H. H. Zhang[23], H. Y. Zhang[1], J. W. Zhang[1], J. Y. Zhang[1], J. Z. Zhang[1], L. Zhang[16], S. H. Zhang[1], X. Y. Zhang[20], Y. Zhang[1], Y. H. Zhang[1], Z. P. Zhang[31], C. Zhao[31], H. S. Zhao[1], Jiawei Zhao[31], Jingwei Zhao[1], Lei Zhao[31], Ling Zhao[1], M. G. Zhao[17], Q. Zhao[1], S. J. Zhao[36], T. C. Zhao[33], X. H. Zhao[16], Y. B. Zhao[1], Z. G. Zhao[31], A. Zhemchugov[13a], B. Zheng[1], J. P. Zheng[1], Y. H. Zheng[6], Z. P. Zheng[1], B. Zhong[15], J. Zhong[2], L. Zhou[1], Z. L. Zhou[1], C. Zhu[1], K. Zhu[1], K. J. Zhu[1], Q. M. Zhu[1], X. W. Zhu[1], Y. S. Zhu[1], Z. A. Zhu[1], J. Zhuang[1], B. S. Zou[1], J. H. Zou[1], J. X. Zuo[1], P. Zweber[30]

(BESIII Collaboration)

[1] *Institute of High Energy Physics, Beijing 100049, P. R. China*

[2] *Bochum Ruhr-University, 44780 Bochum, Germany*

[3] *Carnegie Mellon University, Pittsburgh, PA 15213, USA*

[4] *China Center of Advanced Science and Technology, Beijing 100190, P. R. China*

[5] *G.I. Budker Institute of Nuclear Physics SB RAS (BINP), Novosibirsk 630090, Russia*

[6] *Graduate University of Chinese Academy of Sciences, Beijing 100049, P. R. China*

[7] *GSI Helmholtzcentre for Heavy Ion Research GmbH, D-64291 Darmstadt, Germany*

[8] *Guangxi Normal University, Guilin 541004, P. R. China*

[9] *Guangxi University, Naning 530004, P. R. China*

[10] *Henan Normal University, Xinxiang 453007, P. R. China*

[11] *Huazhong Normal University, Wuhan 430079, P. R. China*

[12] *Hunan University, Changsha 410082, P. R. China*

[13] *Joint Institute for Nuclear Research, 141980 Dubna, Russia*

[14] *Liaoning University, Shenyang 110036, P. R. China*

[15] *Nanjing Normal University, Nanjing 210046, P. R. China*

[16] *Nanjing University, Nanjing 210093, P. R. China*

[17] *Nankai University, Tianjin 300071, P. R. China*

[18] *Peking University, Beijing 100871, P. R. China*

[19] *Seoul National University, Seoul, 151-747 Korea*

[20] *Shandong University, Jinan 250100, P. R. China*

[21] *Shanxi University, Taiyuan 030006, P. R. China*

[22] *Sichuan University, Chengdu 610064, P. R. China*

[23] *Sun Yat-Sen University, Guangzhou 510275, P. R. China*

[24] *The Chinese University of Hong Kong, Shatin, N.T., Hong Kong.*

[25] *The University of Hong Kong, Pokfulam, Hong Kong*

[26] *The University of Tokyo, Tokyo 113-0033 Japan*

[27] *Tsinghua University, Beijing 100084, P. R. China*

[28] *Universitaet Giessen, 35392 Giessen, Germany*

[29] *University of Hawaii, Honolulu, Hawaii 96822, USA*

[30] *University of Minnesota, Minneapolis, MN 55455, USA*

[31] *University of Science and Technology of China, Hefei 230026, P. R. China*

[32] *University of Turin and INFN, Turin, Italy*

[33] *University of Washington, Seattle, WA 98195, USA*

[34] *Wuhan University, Wuhan 430072, P. R. China*

[35] *Zhejiang University, Hangzhou 310027, P. R. China*

[36] *Zhengzhou University, Zhengzhou 450001, P. R. China*

[a] *also at the Moscow Institute of Physics and Technology, Moscow, Russia*

[b] *on leave from the Bogolyubov Institute for Theoretical Physics, Kiev, Ukraine*

[c] *also at the PNPI, Gatchina, Russia*

[d] *currently at Suzhou University, Suzhou 215006, P. R. China*

(Dated: February 12, 2010)

Abstract

Using a sample of 1.06×10^8 ψ' decays collected by the BESIII detector, χ_{c0} and χ_{c2} decays into $\pi^0\pi^0$ and $\eta\eta$ are studied. The branching fraction results are $Br(\chi_{c0} \to \pi^0\pi^0) = (3.23 \pm 0.03 \pm 0.23 \pm 0.14) \times 10^{-3}$, $Br(\chi_{c2} \to \pi^0\pi^0) = (8.8 \pm 0.2 \pm 0.6 \pm 0.4) \times 10^{-4}$, $Br(\chi_{c0} \to \eta\eta) = (3.44 \pm 0.10 \pm 0.24 \pm 0.2) \times 10^{-3}$, and $Br(\chi_{c2} \to \eta\eta) = (6.5 \pm 0.4 \pm 0.5 \pm 0.3) \times 10^{-4}$, where the uncertainties are statistical, systematic due to this measurement, and systematic due to the branching fractions of $\psi' \to \gamma\chi_{cJ}$, respectively. The results provide information on the decay mechanism of χ_c states into pseudoscalars.

PACS numbers: 13.25.Gv, 14.40.Pq

I. INTRODUCTION

In the quark model, the χ_{cJ} ($J = 0, 1, 2$) mesons are $L = 1$ $c\bar{c}$ states. Since they cannot be produced directly in e^+e^- collisions, they are not as well studied as the ψ states. On the other hand, $\psi' \to \gamma\chi_{cJ}$ decays yield many χ_{cJ} mesons, providing a clean environment for χ_{cJ} investigations. In this paper, we study two-body decays of the χ_{c0} and χ_{c2} into $\pi^0\pi^0$ and $\eta\eta$ final states[1]. Knowledge gained from these decays provides information on both the χ_{cJ} parents and their pseudo-scalar daughters, as well as a greater understanding of the decay mechanisms of χ_{cJ} mesons [1].

Recently, χ_{c0} and χ_{c2} decays into two-meson final states were studied by the CLEOc collaboration [2]. In this analysis, we use a sample of 1.06×10^8 ψ' decays collected by the BESIII detector to perform a study of these decays.

II. BESIII AND BEPCII

The analysis reported here is based on about 1.06×10^8 ψ' events collected by BESIII at BEPCII. BEPCII/BESIII [3] is a major upgrade of the BESII experiment at the BEPC accelerator [4] for studies of hadron spectroscopy and τ-charm physics [5]. The design peak luminosity of the double-ring e^+e^- collider, BEPCII, is 10^{33} cm$^{-2}s^{-1}$ at a beam current of 0.93 A. The BESIII detector with a geometrical acceptance of 93% of 4π, consists of the following main components: 1) a small-celled, helium-based main draft chamber (MDC) with 43 layers. The average single wire resolution is 135 μm, and the momentum resolution for 1 GeV/c charged particles in a 1 T magnetic field is 0.5%; 2) an electromagnetic calorimeter (EMC) made of 6240 CsI (Tl) crystals arranged in a cylindrical shape (barrel) plus two endcaps. For 1.0 GeV photons, the energy resolution is 2.5% in the barrel and 5% in the endcaps, and the position resolution is 6 mm in the barrel and 9 mm in the endcaps; 3) a Time-Of-Flight system (TOF) for particle identification composed of a barrel part made of two layers with 88 pieces of 5 cm thick, 2.4 m long plastic scintillators in each layer, and two endcaps with 96 fan-shaped, 5 cm thick, plastic scintillators in each endcap. The time resolution is 80 ps in the barrel, and 110 ps in the endcaps, corresponding to better than a 2 sigma K/pi separation for momenta below about 1 GeV/c; 4) a muon chamber system

[1] We do not consider χ_{c1} decays into these final states, as they are forbidden by spin-parity conservation.

(MUC) made of 1000 m^2 of Resistive Plate Chambers (RPC) arranged in 9 layers in the barrel and 8 layers in the endcaps and incorporated in the return iron of the superconducting magnet. The position resolution is about 2 cm.

The optimization of the event selection and the estimation of physics backgrounds are performed through Monte Carlo simulations. The GEANT4-based simulation software BOOST [6] includes the geometric and material description of the BESIII detectors, the detector response and digitization models, as well as the tracking of the detector running conditions and performance. The production of the ψ' resonance is simulated by the Monte Carlo event generator KKMC [7], while the decays are generated by EvtGen [8] for known decay modes with branching ratios being set to the PDG [10] world average values, and by Lundcharm [9] for the remaining unknown decays. The analysis is performed in the framework of the BESIII Offline Software System (BOSS) [11] which takes care of the detector calibration, event reconstruction and data storage.

III. EVENT SELECTION

A photon candidate is defined as a shower in the EMC with an energy deposit exceeding 50 MeV. The π^0 and η candidates are reconstructed from pairs of photon candidates, using the average event vertex of each run as the assumed origin of the photons. For $\pi^0 \to \gamma\gamma$, the $\gamma\gamma$ invariant mass is required to satisfy $0.075\ \mathrm{GeV}/c^2 < M(\gamma\gamma) < 0.175\ \mathrm{GeV}/c^2$. For $\eta \to \gamma\gamma$, the $\gamma\gamma$ invariant mass is required to satisfy $0.458\ \mathrm{GeV}/c^2 < M(\gamma\gamma) < 0.608\ \mathrm{GeV}/c^2$. The decay angle of a photon is the polar angle measured in the π^0 or η rest frame with respect to the π^0 or η direction in the ψ' rest frame. Real π^0 and η mesons decay isotropically, and their angular distributions are flat. However, the π^0 and η candidates that originate from a wrong photon combination do not have a flat distribution in this variable. To remove wrong photon combinations, the decay angle is required to satisfy $|\cos\theta_{decay}| < 0.95$.

Candidate events for the final states of interest ($\gamma\pi^0\pi^0$ and $\gamma\eta\eta$) are selected using the following basic selection criteria. An event must have 5 or 6 photons and no charged tracks. All possible two photon pairings (the radiative photon from the ψ' decay which has $E < 0.4$ GeV is excluded) in the event are used to form π^0 and η candidates. The candidate event uses the photon pairings giving the minimum

$$\chi_{\pi^0\pi^0/\eta\eta} = \sqrt{P_1^2(\pi^0/\eta) + P_2^2(\pi^0/\eta)},$$

with P_1 and P_2 being the pulls, defined as:

$$P(\pi^0/\eta) = \left[M_{\gamma\gamma} - m_{\pi^0/\eta}\right]/\sigma_{\gamma\gamma},$$

where $M_{\gamma\gamma}$ is the reconstructed $\gamma\gamma$ invariant mass, $m_{\pi^0/\eta}$ is the known π^0 or η mass [10], and $\sigma_{\gamma\gamma}$ is the $\gamma\gamma$ mass resolution, with typical values of 7 MeV/c^2 for the π^0 and 12 MeV/c^2 for the η. If there is more than one radiative photon candidate (E<0.4 GeV), the one that gives the least $|M_{5\gamma} - m_{\psi'}|$ is used.

Backgrounds with missing final state particles are suppressed by requiring small transverse momentum squared $p^2_{t\gamma}$,

$$p^2_{t\gamma} = 4p^2_{miss}\sin^2(\theta_\gamma/2),$$

where p_{miss} is the missing momentum opposite to the $\pi^0\pi^0$ or $\eta\eta$ system and θ_γ is the angle between the radiative photon and the direction of the missing momentum p_{miss}. The $\gamma\pi^0\pi^0$ events are required to satisfy $p^2_{t\gamma} < 0.04$ (GeV/c)^2, while the $\gamma\eta\eta$ events are required to satisfy $p^2_{t\gamma} < 0.01$ (GeV/c)^2 and $\chi_{\eta\eta} < 4$.

To study the efficiency of the $\psi' \to \gamma\chi_{cJ}, \chi_{cJ} \to \pi^0\pi^0$ and $\chi_{cJ} \to \eta\eta$ selection, Monte Carlo samples for each χ_{cJ} state into each final state are generated using a $(1 + \lambda\cos^2\theta)$ distribution, where θ is the radiative photon angle relative to the positron beam direction, and $\lambda = 1$ for χ_{c0} and $\lambda = 1/13$ for χ_{c2}, in accordance with expectations for E1 transitions. The decay products of the χ_{c0} are generated using a flat angular distribution, while those of the χ_{c2} are generated according to a double correlation function of the polar angles of the mesons measured in the χ_c rest frame relative to the transition photon direction [8, 12]. The efficiencies obtained from the Monte Carlo simulation are shown in Table I.

TABLE I: Efficiencies (in %) obtained from analysis of Monte Carlo generated events.

Mode	χ_{c0}	χ_{c2}
$\pi^0\pi^0$	55.6 ± 0.2	59.8 ± 0.2
$\eta\eta$	40.3 ± 0.2	43.9 ± 0.2

Figure 1 and Figure 2 show comparisons in the χ_{c0} region between data and Monte Carlo simulation for the selection criteria used. The good agreement across the distributions shows that the efficiency estimated from Monte Carlo simulation is reliable.

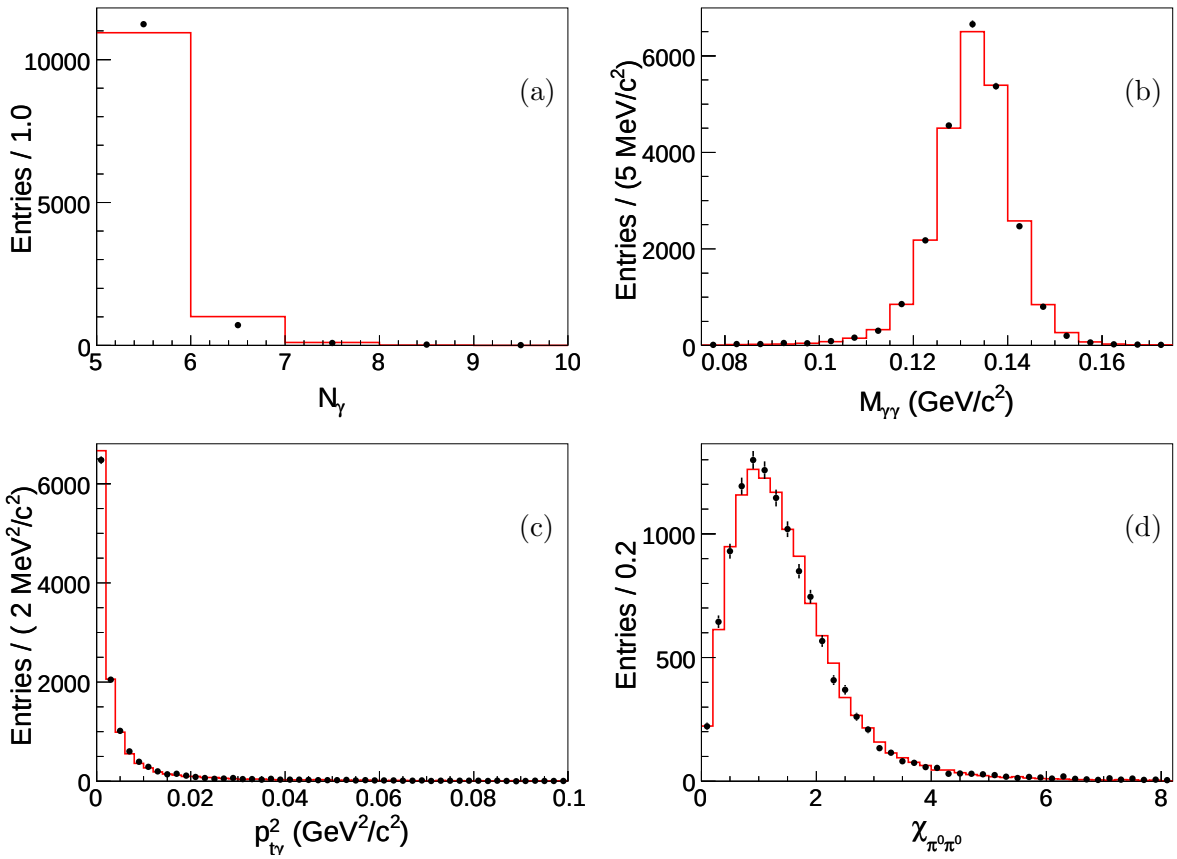

FIG. 1: Comparisons between data and Monte Carlo simulation of $\psi' \to \gamma\chi_{cJ}, \chi_{cJ} \to \pi^0\pi^0$ for selection criteria used. (a) Photon multiplicity distribution. (b) The $\gamma\gamma$ invariant mass distribution for π^0 candidates. (c) The distribution of $p^2_{t\gamma}$. (d) The $\chi_{\pi^0\pi^0}$ distribution. Dots with error bars are data in the χ_{c0} region. The histogram is the Monte Carlo simulation for $\psi' \to \gamma\chi_{c0}, \chi_{c0} \to \pi^0\pi^0$ plus normalized background estimated from inclusive ψ' Monte Carlo samples.

IV. BACKGROUND ANALYSIS

The backgrounds in the selected event sample from a number of potential background channels listed in the PDG [10] are studied with Monte Carlo simulations. The main background to $\chi_{cJ} \to \pi^0\pi^0$ originates from $\psi' \to \gamma\chi_{cJ}$, $\chi_{cJ} \to \gamma J/\psi$, $J/\psi \to \gamma\eta$. Using the world average branching fractions [10] for this mode, we estimate that 48 events from this channel are in the signal region. However, the simulation also shows that the background does not peak at the χ_{c0} nor the χ_{c2} mass region. The main backgrounds to $\chi_{cJ} \to \eta\eta$ originate from $\psi' \to \pi^0\pi^0 J/\psi$ and $\psi' \to \eta J/\psi$, $J/\psi \to \gamma\eta$. There are about 233 surviving background events in the signal region.

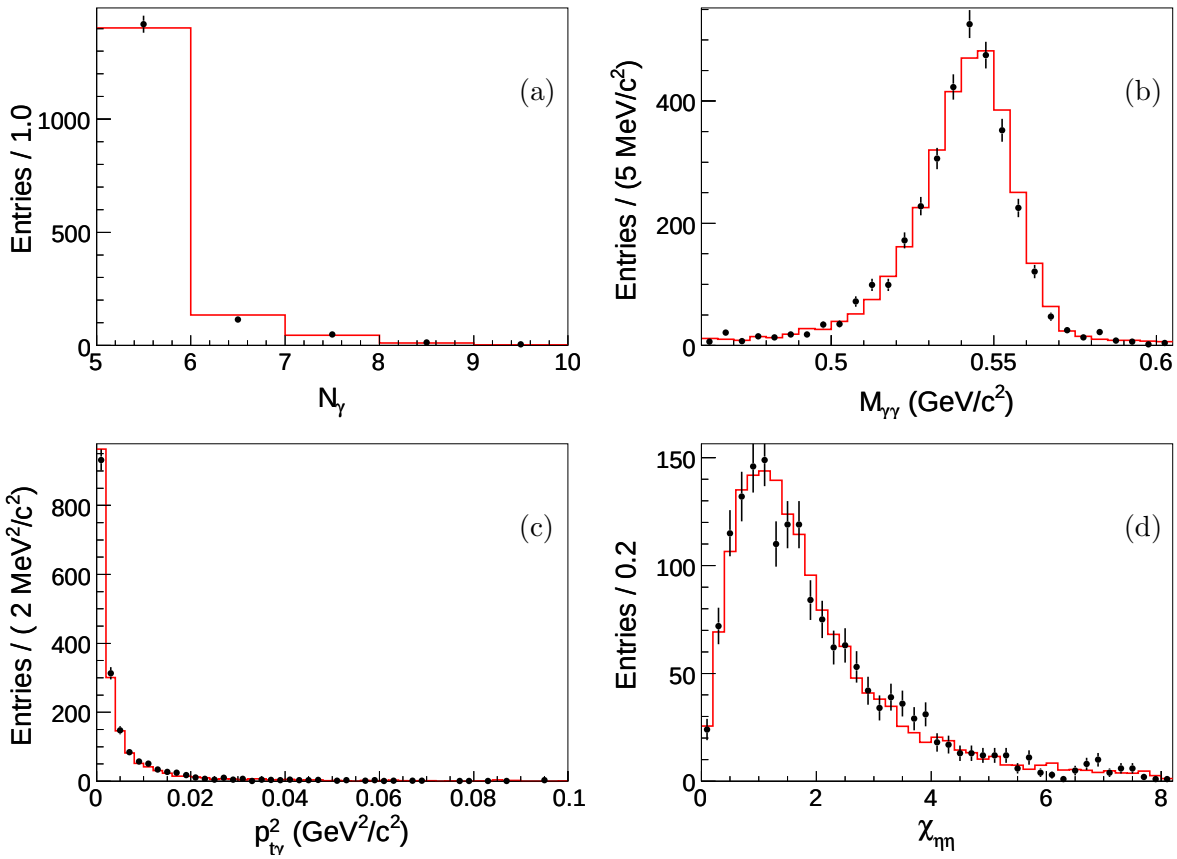

FIG. 2: Comparisons between data and Monte Carlo simulation for $\psi' \to \gamma\chi_{cJ}, \chi_{cJ} \to \eta\eta$ for the selection criteria used. (a) Photon multiplicity distribution. (b) The $\gamma\gamma$ invariant mass distribution for η candidates. (c) The distribution of $p^2_{t\gamma}$. (d) The $\chi_{\eta\eta}$ distribution. Dots with error bars are data in the χ_{c0} region. The histogram is the Monte Carlo simulation for $\psi' \to \gamma\chi_{c0}, \chi_{c0} \to \eta\eta$ plus the normalized background estimated from inclusive ψ' Monte Carlo samples.

A 10^8 inclusive ψ' Monte Carlo event sample is also used to investigate other possible surviving background events. Figs. 3 (a) and 3 (b) show the radiative photon energy distribution of the selected $\chi_{cJ} \to \pi^0\pi^0$ and $\chi_{cJ} \to \eta\eta$ events and the normalized backgrounds estimated with the inclusive ψ' Monte Carlo sample, respectively. In the χ_{cJ} signal region, there is no peaking background from the inclusive ψ' Monte Carlo sample.

The background in our signal region originating from non-resonant processes is studied using a continuum data sample collected at a center of mass energy of 3.65 GeV. Normalized according to the luminosities, the contribution to $\chi_{cJ} \to \pi^0\pi^0$ is 384 events, as shown in Fig. 3 (a), and the contribution to $\chi_{cJ} \to \eta\eta$ is 48 events, as shown in Fig. 3 (b). These

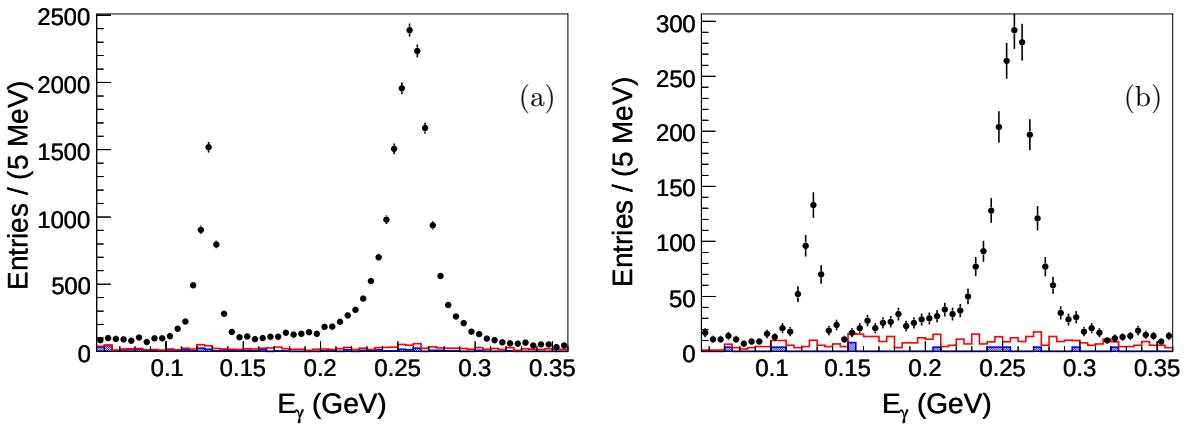

FIG. 3: Radiative photon energy distributions of (a) selected $\chi_c \to \pi^0\pi^0$ events, and (b) selected $\chi_c \to \eta\eta$ events. Dots with error bars are data. The open histogram is the normalized background estimated from the inclusive ψ' Monte Carlo sample and from the continuum. The shaded histogram is the normalized contribution from the continuum.

backgrounds are small, do not peak in the signal region, and are included as part of the polynomial background below.

V. NUMBER OF ψ' EVENTS

The number of ψ' events, $N_{\psi'}$, used in this analysis is determined from the number of inclusive hadronic ψ' decays. Charged tracks are selected requiring their point of closest approach to the beam axis be within 1 cm of the beam line, and their angle with respect to the beam axis, θ, must satisfy $|\cos\theta| < 0.93$. Photon candidates must have at least 25 (50) MeV of energy in the barrel (end-cap) EMC, and have $|\cos\theta| < 0.93$.

Event selection requires at least one charged track. To remove beam associated background and background from Bhabha events, there are special requirements on low charged multiplicity events. For events with one charged track, there must be at least three photons, the acolinearity angle between the two highest energy photons must be greater than 7°, and the total energy in the EMC, E_{EMC}, must be greater than 0.2 of the center of mass energy, E_{cm}, and less than $0.85E_{cm}$. Events with two or three tracks must have $E_{EMC} > 0.2E_{cm}$ in order to suppress beam associated backgrounds. Backgrounds from Bhabha events are reduced by requiring the presence of at least two photons and $E_{EMC} < 0.85E_{cm}$ or the

largest energy deposit in the calorimeter less than 0.85 times the beam energy, E_{beam}. In addition, the second highest momentum track must have momentum less than $0.9E_{beam}$, and the acolinearity angle in the $x-y$ plane of the two highest momentum tracks must be greater than 7°.

The number of hadronic events is determined from the distribution of $\bar{z}$, which is the average of the distances, z, from the interaction point along the beam of the point of closest approach of tracks to the beam line. Two methods are used: fitting the distribution with a Gaussian plus a 2nd order polynomial background and counting events in a signal region and subtracting sideband events. Backgrounds from Bhabha, dimuon, and ditau events surviving the selection criteria are very small. The continuum contribution and the surviving backgrounds are removed by subtracting the number of events selected with the above criteria from a continuum sample taken at a center of mass energy of 3.65 GeV and normalized by relative luminosity and the $1/s$ dependence. The efficiency for $\psi' \to hadrons$ is determined by simulation [7] and is 0.80. The agreement between data and Monte Carlo (MC) simulation is shown for the distribution of the number of charged tracks in Fig. 4 (a) and for E_{EMC} in Fig. 4 (b).

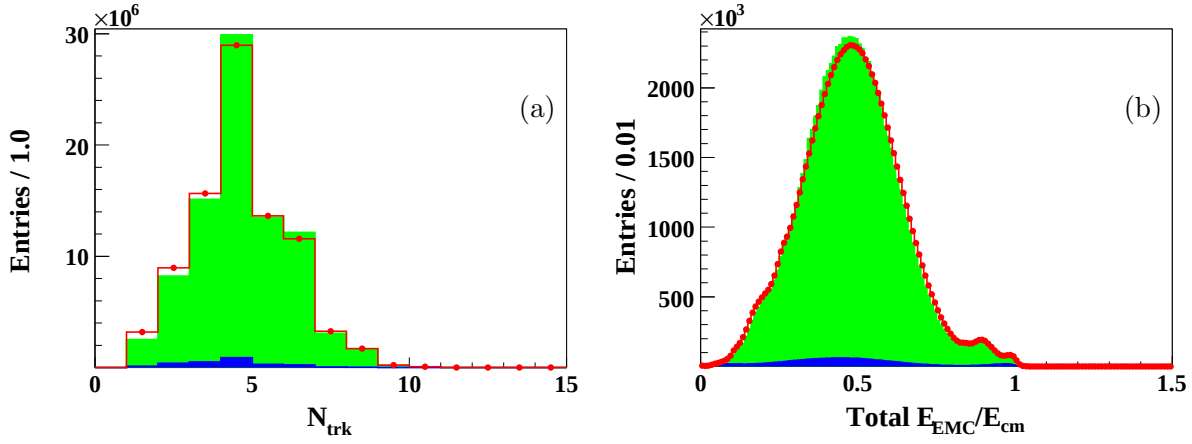

FIG. 4: (a) The distribution of the number of charged tracks for events satisfying selection criteria. (b) The distribution of the total energy in the EMC divided by the center of mass energy, E_{EMC}/E_{cm}, for events satisfying selection criteria. All requirements are applied to events with one to three charged tracks except the EMC requirements. Dots are data, the light shaded histogram is the sum of normalized continuum and $\psi' \to hadrons$ simulated events, and the dark shaded histogram is from continuum data.

The result is $N_{\psi'} = (1.06 \pm 0.04) \times 10^8$, where the error is systematic and is determined mostly by the track efficiency difference between data and MC (1.2%), the variation with the minimum charged track multiplicity requirement (2.86%), the difference when a minimum transverse momemtum requirement is used (0.95%), the uncertainty of the generator model (0.61%), and error due to the continuum subtraction (0.91%). The statistical error is negligible. A second analysis using a much different selection criteria with a higher efficiency determines an almost identical result.

VI. FITTING RESULTS

The $\chi_c \to \pi^0\pi^0$ branching fraction is calculated using

$$Br(\chi_c \to \pi^0\pi^0) = \frac{N_{obs}}{N_{\psi'} \cdot \varepsilon \cdot Br(\psi' \to \gamma\chi_{cJ}) \cdot Br(\pi^0 \to \gamma\gamma) \cdot Br(\pi^0 \to \gamma\gamma)},$$

where N_{obs} is the number of events observed, $N_{\psi'}$ is the number of ψ' events, and ε is the selection efficiency obtained from MC simulation.

The radiative photon energy spectrum of $\chi_{cJ} \to \pi^0\pi^0$ candidates, shown in Fig. 5, is fitted using an unbinned maximum likelihood fit in the range from 0.06 GeV to 0.36 GeV. The shapes of the χ_{c0} and χ_{c2} are obtained from Monte Carlo simulation and the masses and widths of χ_{cJ} are fixed to their PDG values [10]. A 2nd-order Chebychev polynomial is used to describe the backgrounds, including those found in the inclusive MC study and the continuum. The fit gives a χ_{c0} signal yield of 17443 ± 167 events and a χ_{c2} signal yield of 4516 ± 80 events. The selection efficiency from Monte Carlo simulation of $\psi' \to \gamma\chi_{c0}(\chi_{c0} \to \pi^0\pi^0, \pi^0 \to \gamma\gamma)$ is $(55.6 \pm 0.2)\%$ and the efficiency of $\psi' \to \gamma\chi_{c2}(\chi_{c2} \to \pi^0\pi^0, \pi^0 \to \gamma\gamma)$ is $(59.8 \pm 0.2)\%$. The branching fractions are then determined to be

$$Br(\chi_{c0} \to \pi^0\pi^0) = (3.23 \pm 0.03) \times 10^{-3},$$

$$Br(\chi_{c2} \to \pi^0\pi^0) = (8.8 \pm 0.2) \times 10^{-4},$$

where the errors are statistical only.

The fit to the radiative photon energy spectrum of $\chi_{cJ} \to \eta\eta$ candidates, shown in Fig. 6, gives a χ_{c0} signal yield of 2132 ± 60 events and a χ_{c2} signal yield of 386 ± 25 events. The selection efficiency is $40.3 \pm 0.2\%$ and $43.9 \pm 0.2\%$ for $\chi_{c0} \to \eta\eta$ and $\chi_{c2} \to \eta\eta$, respectively.

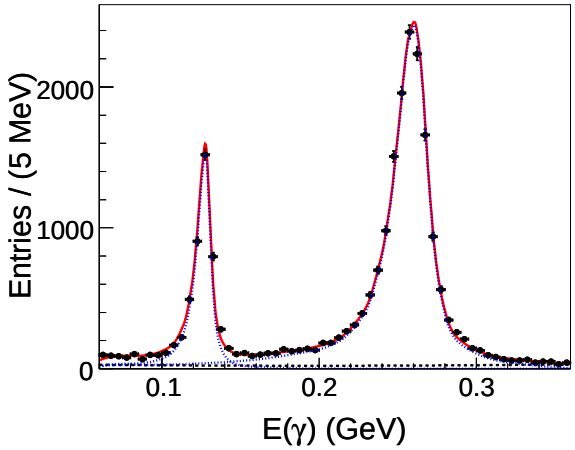

FIG. 5: The radiative photon energy spectrum of selected $\chi_c \to \pi^0\pi^0$ events. Dots with error bars are data. The solid curve is the result of a fit described in the text. The dotted curves are the χ_{cJ} signals. The dashed curve is the background polynomial.

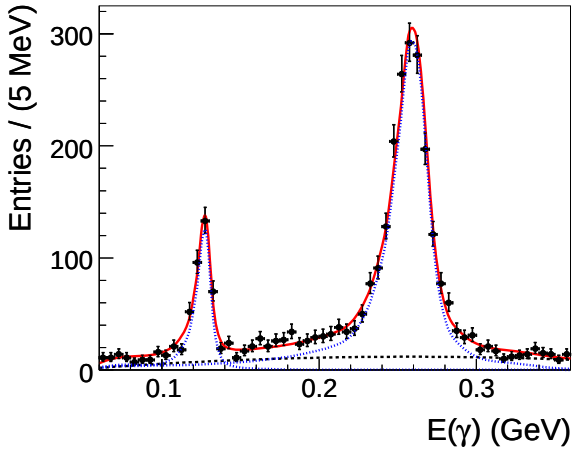

FIG. 6: The radiative photon energy spectrum of selected $\chi_c \to \eta\eta$ events. Dots with error bars are data. The solid curve is the result of a fit described in the text. The dotted curves are the χ_{cJ} signals. The dashed curve is the background polynomial.

The branching fractions are

$$Br(\chi_{c0} \to \eta\eta) = (3.44 \pm 0.10) \times 10^{-3},$$

$$Br(\chi_{c2} \to \eta\eta) = (6.5 \pm 0.4) \times 10^{-4},$$

where the errors are statistical only.

VII. SYSTEMATIC UNCERTAINTIES

The systematic uncertainties on the branching fractions come from many different sources and are summarized in Table II. The uncertainty due to photon detection and photon conversion is 1% per photon. This is determined from studies of photon detection efficiencies in well understood decays such as $J/\psi \to \rho^0\pi^0$ and study of photon conversion via $e^+e^- \to \gamma\gamma$.

The uncertainty due to π^0 selection is determined from a high purity control sample of $J/\psi \to \pi^+\pi^-\pi^0$ decays. The π^0 selection efficiency is obtained from the change in the π^0 yield in the $\pi^+\pi^-$ recoiling mass spectrum with or without the π^0 selection requirement. The difference of π^0 reconstruction efficiency between data and Monte Carlo simulation gives an uncertainty of 1% per π^0. The uncertainty from the η selection is 1% per η, which is determined in a similar way from a high purity control sample of $J/\psi \to \eta p\bar{p}$.

The systematic error from the $p^2_{t\gamma}$ requirement is determined by not using the requirement. The change in the yield gives systematic errors of 0.9% for $\chi_{c0} \to \pi^0\pi^0$, 1.2% for $\chi_{c2} \to \pi^0\pi^0$, 0.1% for $\chi_{c0} \to \eta\eta$, and 0.3% for $\chi_{c2} \to \eta\eta$. The uncertainties from $\chi_{\eta\eta}$ requirement are 0.6% for $\chi_{c0} \to \eta\eta$ and 2.6% for $\chi_{c2} \to \eta\eta$, and are determined in a similar way.

Since the shapes of the signals in the fit are obtained from Monte Carlo simulation, their uncertainties are estimated by changing the masses and widths of χ_{cJ} by one standard deviation from the PDG values [10] and taking into account the uncertainties of the photon energy scale and resolution in the Monte Carlo simulation. They are 1.6% for $\chi_{c0} \to \pi^0\pi^0$, 1.2% for $\chi_{c2} \to \pi^0\pi^0$, 1.4% for $\chi_{c0} \to \eta\eta$, and 1.5% $\chi_{c2} \to \eta\eta$.

The background uncertainties are evaluated by changing the background fitting function from a second order polynomial to third order, resulting in changes of branching ratios by 0.5% for $\chi_{c0} \to \pi^0\pi^0$, 0.5% for $\chi_{c2} \to \pi^0\pi^0$, 0.2% for $\chi_{c0} \to \eta\eta$, and 0.3% for $\chi_{c2} \to \eta\eta$.

The systematic uncertainties due to the fitting of the radiative photon energy spectrum were evaluated by changing the fitting range from (0.05, 0.37) GeV to (0.07, 0.35) GeV. The change in yield for this variation gives systematic uncertainties of 0.3% for $\chi_{c0} \to \pi^0\pi^0$, 0.3% for $\chi_{c2} \to \pi^0\pi^0$, 0.8% for $\chi_{c0} \to \eta\eta$, and 1.3% for $\chi_{c2} \to \eta\eta$.

The systematic uncertainties due to the trigger efficiency in these neutral channels is estimated to be $< 0.1\%$, based on cross checks using different trigger conditions. The uncertainty on the number of ψ' events is 4%.

The total systematic uncertainties, shown in Table. II, are obtained by adding all the above systematic errors in quadrature. The uncertainty due to the $\psi' \to \gamma\chi_c$ branching fractions is kept separate and quoted as a second systematic uncertainty.

TABLE II: Systematic uncertainties expressed in percent.

Mode	$\chi_{c0} \to \pi^0\pi^0$	$\chi_{c2} \to \pi^0\pi^0$	$\chi_{c0} \to \eta\eta$	$\chi_{c2} \to \eta\eta$
photon detection	5	5	5	5
$\pi^0(\eta)$ reconstruction	2	2	2	2
$p^2_{t\gamma}$	0.9	1.2	0.1	0.3
$\chi_{\eta\eta}$	-	-	0.6	2.6
signal shape	1.6	1.2	1.4	1.5
background shape	0.5	0.5	0.2	0.3
fitting range	0.3	0.3	0.8	1.3
trigger	0.1	0.1	0.1	0.1
$N_{\psi'}$	4	4	4	4
Total	7.0	6.9	6.9	7.5

TABLE III: Branching fraction results (in units of 10^{-3}) for each decay mode. The uncertainties are statistical, systematic due to this measurement, and systematic due to the branching fractions of $\psi' \to \gamma\chi_{cJ}$, respectively. CLEOc results are determined using their own branching fractions for $\psi' \to \gamma\chi_{cJ}$, while ours are determined using branching fractions from the PDG. If we use the CLEOc branching fractions, we find $Br(\chi_{c0} \to \pi^0\pi^0) = 3.29 \times 10^{-3}$, $Br(\chi_{c0} \to \eta\eta) = 3.51 \times 10^{-3}$, $Br(\chi_{c2} \to \pi^0\pi^0) = 0.78 \times 10^{-3}$, and $Br(\chi_{c2} \to \eta\eta) = 0.58 \times 10^{-3}$.

Mode		χ_{c0}	χ_{c2}
$\pi^0\pi^0$	This Work	$3.23 \pm 0.03 \pm 0.23 \pm 0.14$	$0.88 \pm 0.02 \pm 0.06 \pm 0.04$
	CLEOc [2]	$2.94 \pm 0.07 \pm 0.32 \pm 0.15$	$0.68 \pm 0.03 \pm 0.07 \pm 0.04$
	PDG [10]	2.43 ± 0.20	0.71 ± 0.08
$\eta\eta$	This Work	$3.44 \pm 0.10 \pm 0.24 \pm 0.13$	$0.65 \pm 0.04 \pm 0.05 \pm 0.03$
	CLEOc [2]	$3.18 \pm 0.13 \pm 0.31 \pm 0.16$	$0.51 \pm 0.05 \pm 0.05 \pm 0.03$
	PDG [10]	2.4 ± 0.4	< 0.5

VIII. SUMMARY

In summary, with a sample of 1.06×10^8 ψ' events in the BESIII detector, improved measurements of the branching fractions of $\chi_{c0,2} \to \pi^0\pi^0$ and $\chi_{c0,2} \to \eta\eta$ are performed: $Br(\chi_{c0} \to \pi^0\pi^0) = (3.23 \pm 0.03 \pm 0.23 \pm 0.14) \times 10^{-3}$, $Br(\chi_{c2} \to \pi^0\pi^0) = (8.8 \pm 0.2 \pm 0.6 \pm 0.4) \times 10^{-4}$, $Br(\chi_{c0} \to \eta\eta) = (3.44 \pm 0.10 \pm 0.24 \pm 0.2) \times 10^{-3}$, and $Br(\chi_{c2} \to \eta\eta) = (6.5 \pm 0.4 \pm 0.5 \pm 0.3) \times 10^{-4}$, where the uncertainties are statistical, systematic due to this measurement, and systematic due to the branching fractions of $\psi' \to \gamma\chi_{cJ}$, respectively. Results are listed in Table III and compared with previous measurements.

IX. ACKNOWLEDGMENTS

The BESIII collaboration thanks the staff of BEPC and the computing center for their hard efforts. This work is supported in part by the Ministry of Science and Technology of China under Contract No. 2009CB825200; National Natural Science Foundation of China (NSFC) under Contracts Nos. 10625524, 10821063, 10825524, 10835001, 10935007; the Chinese Academy of Sciences (CAS) Large-Scale Scientific Facility Program; CAS under Contracts Nos. KJCX2-YW-N29, KJCX2-YW-N45; 100 Talents Program of CAS; Istituto Nazionale di Fisica Nucleare, Italy; Russian Foundation for Basic Research under Contracts Nos. 08-02-92221, 08-02-92200-NSFC-a; Siberian Branch of Russian Academy of Science, joint project No 32 with CAS; the Chinese University of Hong Kong Focused Investment Grant under Contract No. 3110031; U. S. Department of Energy under Contracts Nos. DE-FG02-04ER41291, DE-FG02-91ER40682, DE-FG02-94ER40823; WCU Program of National Research Foundation of Korea under Contract No. R32-2008-000-10155-0. D. Cronin-Hennessy thanks the A.P. Sloan Foundation. This paper is also supported by the NSFC under Contract Nos. 10979038, 10875113.

[1] Q. Zhao, Phys. Rev. D **72**, 074001 (2005).

[2] D. M. Asner *et al.* (CLEO Collaboration), Phys. Rev. D **79**, 072007 (2009)

[3] M. Ablikim, *et al.*, Design and construction of the BESIII detector, arXiv:0911.4960, to appear in Nucl. Instrum. Meth. A

[4] J. Z. Bai *et al.* (BES Collaboration), Nucl. Instrum. Meth. A **344**, 319 (1994); Nucl. Instrum. Meth. A **458**, 627 (2001).

[5] "Physics at BESIII", Edited by K. T. Chao and Y. F. Wang, Int. J. Mod. Phys. A **24**, No.1 (2009) supp.

[6] Z.Y. Deng *et al.*, Chinese Physics C **30** (2006) 371.

[7] S. Jadach, B. F. L. Ward and Z. Was, Comput. Phys. Commun. **130**, 260 (2000); Phys. Rev. D **63**, 113009 (2001)

[8] R.G. Ping *et al.*, Chinese Physics C **32** (2008) 599.

[9] J. C. Chen, G. S. Huang, X. R. Qi, D. H. Zhang and Y. S. Zhu, Phys. Rev. D **62**, 034003 (2000).

[10] C. Amsler *et al.* (Particle Data Group), Phys. Lett. B **667**, 1 (2008).

[11] W.D Li, H.M Liu *et al.*, The Offline Software for the BESIII Experiment, Proceeding of CHEP 2006.

[12] P.K. Kumar and A.J.G. Hey, Phys. Rev. D **13**, 3161 (1976).